UCRL-BOOK-217328

LAWRENCE
LIVERMORE
NATIONAL
LABORATORY

Reconstructing Past Ocean Salinity ((delta)18Owater)

T. P. Guilderson, D. K. Pak

November 29, 2005

Encyclopedia of Quaternary Science

This document was prepared as an account of work sponsored by an agency of the United States Government. Neither the United States Government nor the University of California nor any of their employees, makes any warranty, express or implied, or assumes any legal liability or responsibility for the accuracy, completeness, or usefulness of any information, apparatus, product, or process disclosed, or represents that its use would not infringe privately owned rights. Reference herein to any specific commercial product, process, or service by trade name, trademark, manufacturer, or otherwise, does not necessarily constitute or imply its endorsement, recommendation, or favoring by the United States Government or the University of California. The views and opinions of authors expressed herein do not necessarily state or reflect those of the United States Government or the University of California, and shall not be used for advertising or product endorsement purposes.

Updated October 14, 2003

Reconstructing Past Ocean Salinity ($\delta^{18}O_{water}$)

T.P. Guilderson[1,3] & D.K. Pak[2]
[1]Center for Accelerator Mass Spectrometry, UC/LLNL, Livermore CA 94550
[2]Department of Earth Science and Marine Science Institute, UC-Santa Barbara, Santa Barbara CA 93106
[3]Department of Ocean Sciences and Institute of Marine Sciences, UC-Santa Cruz, Santa Cruz CA 95064

---

1. Introduction

Temperature and salinity are two of the key properties of ocean water masses. The distribution of these two independent but related characteristics reflects the interplay of incoming solar radiation (insolation) and the uneven distribution of heat loss and gain by the ocean, with that of precipitation, evaporation, and the freezing and melting of ice. Temperature and salinity to a large extent, determine the density of a parcel of water. Small differences in temperature and salinity can increase or decrease the density of a water parcel, which can lead to convection. Once removed from the surface of the ocean where "local" changes in temperature and salinity can occur, the water parcel retains its distinct relationship between (potential) temperature and salinity. We can take advantage of this "conservative" behavior where changes only occur as a result of mixing processes, to track the movement of water in the deep ocean (Figure 1). The distribution of density in the ocean is directly related to horizontal pressure gradients and thus (geostrophic) ocean currents. During the Quaternary when we have had systematic growth and decay of large land based ice sheets, salinity has had to change. A quick scaling argument following that of Broecker and Peng [1982] is: the modern ocean has a mean salinity of 34.7 psu and is on average 3500m deep. During glacial maxima sea level was on the order of ~120m lower than present. Simply scaling the loss of freshwater (3-4%) requires an average increase in salinity a similar percentage or to ~35.9psu. Because much of the deep ocean is of similar temperature, small changes in salinity have a large impact on density, yielding a potentially different distribution of water masses and control of the density driven (thermohaline) ocean circulation. It is partly for this reason that reconstructions of past salinity are of interest to paleoceanographers.

What is salinity? At the simplest of all levels, salinity is the total amount of dissolved materials in seawater. It is not practical to evaporate seawater samples to dryness to determine the total dissolved materials and some materials such as chlorides are lost during drying. A more complete definition was created by the International Council for the Exploration of the Sea whereby salinity was defined as the *"total amount of solid materials in grams dissolved in one kilogram of sea water when all the carbonate has been converted to oxide, the bromine and iodine replaced by chlorine and all organic matter completely oxidized."* Again this is a difficult measurement to make accurately. Taking advantage of the near constant proportionality of the major salts in seawater, salinity was “redefined” using chlorinity and a simple linear relation $S = 1.80655*Cl$, where chlorinity is *“the amount of silver required to precipitate completely the halogens in 0.3285234kg of seawater”* [*Wooster et al.*, 1969]. At about the same time, a relationship between salinity and conductivity was also proposed. Conductivity measurements are relatively easy compared to the chemistry-based techniques, and accurate. The relationship between salinity and conductivity has been revised slightly such that the practical salinity scale of 1978 is now the official definition and knowing the conductivity, pressure, and in situ temperature allows salinity to be calculated [*Joint Panel* 1980; *Millero* 1996]. Surface salinities reflect the precipitation-evaporation-fresh water balance and span the full range of potential values from 0 psu in freshwater rivers and coastal environments to 42psu in regions of high evaporation such as the Red Sea. Interior ocean salinities do not range as much: ~33.8psu (Antarctic Intermediate Water) to ~36.5 (North Atlantic Central Water), with abyssal waters in general differing by less than 1 psu (Figure 2).

2. Reconstructing Past Salinity Variations (with an emphasis on the Quaternary)

As paleoceanographers we have several different approaches that we can utilize to reconstruct past variations in salinity. These can be grossly classified as “biological” and “chemical.” In the purely biological approach we relate the distribution and relative abundance of certain species to salinity and make an assumption that this empirical relationship holds back through time. The salinity gradients in the deep ocean are very small so this approach has been mainly used to attempt to reconstruct surface salinity variations in the open ocean, and changes in estuarine or coastal environments. A classic example of this approach is the work of CLIMAP researchers [*e.g.*, *Kipp* 1976] who related the distribution of planktonic foraminifera in core-top sediments to seasonal and annual salinity. In this example, the relative abundances of the (26) species of planktonic foraminifera are deconstructed using Q-mode factor analysis [*e.g., Imbrie and Kipp* 1971; *Joreskog et al.,* 1976] into major modes or factors which are then related to surface salinity observations using a multiple linear regression scheme (Figure 3). The empirically derived relationship between the major factors and salinity is then used as a model to estimate past surface salinity from planktonic foraminifera census counts in sediment samples taken downcore and back through time (Figure 4).

How might we otherwise reconstruct past salinity variations and take advantage of other “conventional” biogeochemical proxies? Are there relationships between elements or isotopes in the skeletons of for example carbonate fossils and salinity? Can we directly measure past salinity variations?

2.1 “Current” methods of reconstructing past salinity

Current methods of reconstructing past ocean salinity focus on using either direct measurements of past $\delta^{18}O_{water}$ (*e.g.*, glacial pore water $\delta^{18}O$), or independent paleotemperature proxies (*e.g.*, alkenones, foraminiferal Mg/Ca, coral Sr/Ca, faunal assemblages) to extract the past $\delta^{18}O_{water}$ signal from the $\delta^{18}O$-carbonate record. Pore water chlorinity measurements can be used to directly estimate glacial salinity. The indirect methods using biogeochemical proxies have the advantage over the direct pore water estimates by facilitating time series and having the potential to document so-called abrupt climate change events at the sub-millennial to seasonal time-scale. The reconstructed $\delta^{18}O_{water}$ record can then be deconvolved into its ice volume and salinity components. For the sake of this paper, we focus on open ocean salinity changes, although additional methods of reconstructing estuarine and brackish water salinities are used. For example, the large salinity changes associated with brackish environments allows the use of faunal assemblage changes as direct salinity proxies, whereas in open ocean environments salinity changes are generally too subtle to cause large faunal changes. We focus particularly on combining Mg/Ca and $\delta^{18}O$ measurements in marine carbonates as a means to reconstruct open ocean glacial-interglacial $\delta^{18}O_w$ (salinity) estimates. An analogous technique applied to reef-building hermatypic corals is the combination of Sr/Ca and $\delta^{18}O$ [*c.f. McCulloch et al., 1994; Hendy et al., 2002; Quinn* this volume;].

We begin with the consideration of the workhorse of paleoceanography: $\delta^{18}O$ thermometry. We do this because the direct estimates of salinity during the last glaciation provide a constraint on one of the primary factors in the $\delta^{18}O$ of marine carbonate and thus there is a need to have common basis of understanding. The ratio of ^{18}O to ^{16}O (expressed as $\delta^{18}O$) in biogenic carbonates has been exploited as a geochemical paleothermometer since the pioneering work of *Urey* [1947, 1953] and *Epstein* [1951, 1953]. *Weber and Woodhead* [1972] documented that the oxygen isotope temperature sensitivity of reef-building hermatypic corals is similar to that of the oxygen paleotemperature scale developed for mollusks [*McCrea*, 1950; *Urey et al.*, 1951; *Epstein et al.*, 1951, 1953], approximately 0.21‰ per °C. Similar comparisons have been made using foraminifera [*eg., Bemis et al.*, 1998, *Shackelton* 1974 among many]. Thus biogenic carbonate $\delta^{18}O$ is a function of temperature, and variations in the oxygen isotopic composition of water (δ_W). (To be complete, carbonate ion content and pH also exert a small effect – *Spero et al* 1997. For this discussion we will assume that this is a minor effect.) Most marine biogenic carbonate materials have a temperature sensitivity similar to that of inorganic carbonate [*e.g., Kim and O'Neil* 1997].

So what controls the oxygen isotopic composition of seawater and does this relate back to salinity? On long, geologic timescales water-rock interactions control the mean isotopic composition [*Faure 1986*]. On glacial-interglacial timescales ^{18}O depleted water is locked up in ice sheets leaving the ocean more enriched in ^{18}O. In a gross oversimplification ^{18}O is heavier than its more abundant ^{16}O cousin and as moisture travels from the evaporating sources of the ocean to the growing ice sheet the ^{18}O rains out in precipitation leaving the remaining vapor depleted or more negative (*cf. Craig and Gordon* 1965; *Dansgaard* 1964; *Rozanski et al.*, 1993 Figure 5), this is in addition to the lower vapor pressure of ^{18}O which yields a more negative (fewer $H_2{}^{18}O$ than $H_2{}^{16}O$ compared to the water source) vapor phase to begin with. Thus during glacial periods when this high latitude precipitation is locked up in ice-sheets the ocean has more ^{18}O in it than during interglacials or if you prefer, less ^{16}O, which leaves the ocean relatively "enriched" in ^{18}O with a corresponding more positive $\delta^{18}O_W$. Even without growing ice-sheets, high latitude (and altitude) precipitation has a more negative δ^{18}O value and as this water enters the ocean as freshwater with zero salinity it yields a relationship between salinity and $\delta^{18}O_W$. *Craig and Gordon* [1965] proffered the first ocean-wide or global surface salinity-$\delta^{18}O_W$ relationship: ~0.6‰ for every salinity unit (Figure 6a). In actuality, the whole ocean salinity-$\delta^{18}O_W$ relationship is the result of a series of regional relationships (Figure 6b and c) which reflect the local precipitation-evaporation balance, the input of river or glacial meltwater, and ocean dynamics [*eg., Fairbanks et al.*, 1992; *Schmidt et al.* 1999]. Local/regional surface water $\delta^{18}O_w$-salinity relations range by an order of magnitude from ~0.2‰/psu to ~1.5‰/psu (Figure 6c). The deep-ocean $\delta^{18}O_w$salinity relationship is on the order of ~1.5‰/psu [*e.g., Craig and Gordon*, 1965].

If one can independently determine or estimate temperature and the eustatic (global) ice-volume component, these can be converted into δ^{18}O space and subtracted from the measured (biogenic) $\delta^{18}O_{carbonate}$. The residual δ^{18}O is an estimate of regional δ_W (salinity) variations. Implicitly, it is assumed that the regional relationships determined on present day seawater hold back through time. During the late Holocene and in the "near instrumental" period, there is no ice volume component. In theory, this allows for a simple subtraction of the temperature component from measured $\delta^{18}O_{carbonate}$. Late Holocene and near instrumental paleosalinity (δ_w) studies include seasonal and interannual variability of freshwater input on the Great Barrier Reef as a consequence of the El Niño-Southern Oscillation, and surface salinity variations of the North and subtropical Atlantic during the Little Ice Age to name a few.

So called "site to site" δ^{18}O reconstructions can in principle avoid many of the complications of deconvolving ice volume and temperature from individual cores' marine carbonate δ^{18}O. An example of this is the work of Maslin and Burns [2000] who utilized a suite of cores off the coast of Brasil to estimate the past (salinity) influence of the Amazon outflow. In this example a set of cores was selected from a limited geographical area where it was expected that each core site had similar past sea surface temperature variations. One set of cores was south and upstream of where the Amazon River discharges into the Western Equatorial Atlantic and the other set was downstream of the discharge point. The records were independently synchronized (*eg*., ^{14}C dates and/or a stratigraphic tool other than δ^{18}O). The common portion of their δ^{18}O signal includes ice volume and sea surface temperature. The non-common portion is the difference in sea surface $\delta^{18}O_w$ (salinity) due to the Amazon. Subtraction of the downstream core's planktonic δ^{18}O timeseries from that of the upstream one yielded a time-varying estimate of the influence of the Amazon.

In a series of elegant studies, *Schrag et al.*, [1996] and *Adkins et al.*, [2002] analyzed the δ^{18}O content of deep-ocean sediment porewaters and determined that the mean ocean was ~1‰ heavier during the last glacial maximum. Over time via diffusive processes pore-water δ^{18}O equilibrates with that of the overlying deep-ocean. Thus the change from full glacial conditions ~20,000 years ago to the present interglacial is "remembered" in the sediments. Combining measurements with a pore-water diffusion model allows the glacial condition to be reconstructed from the current porewater $\delta^{18}O_w$ profile. To do so they compressed or squeezed the pore-waters out of sediment and analyzed its oxygen isotopic composition. These results provide a direct measure of removing the whole ocean $\delta^{18}O_w$ from marine carbonate $\delta^{18}O$ analyses. This change can then be partitioned as a function of sea level (time) over the last glacial cycle in a fashion similar to that proposed by *Fairbanks and Matthews* [1979] and *Fairbanks* [1989; 1990]. It is generally assumed that this relation holds for previous Pleistocene glacial cycles and mainly insensitive to the oxygen isotope composition of Northern versus Southern hemisphere ice sheets [*eg., Mix*, 1987]. Adkins, McIntyre, and Schrag [2002] performed a more difficult suite of porewater chlorinity measurements thus providing for the first time a direct measure of salinity of the deep ocean during the last glacial maximum. *Adkins et al.*, confirmed that the deep ocean was significantly saltier 20,000 years ago and that the deep ocean was significantly colder than present (Figure 7). Astonishingly, *Adkins et al.*, measured waters from the deep Southern and Pacific oceans that are significantly more salty than our whole ocean glacial estimate of 35.9psu. They determined that unlike today when the saltiest deep-water is formed in the North Atlantic, the Southern Ocean was saltier by a large margin. *Adkins et al.*, correctly infer that brine rejection during sea-ice formation played a much more dominant role in deep-water production. A corollary to this observation is that the pole to pole freshwater budget must have been very different than today. A very strong constraint on the mechanisms of formation and redistribution of deep-water during the last glaciation would be a systematic basin-wide porewater study similar to *Adkins et al.*, to accurately constrain the geometry of glacial deep-waters. This direct reconstruction of paleosalinity (through chlorinity) removes assumptions and complications due to nutrient chemistry implicit in other biogeochemical proxies such as $\delta^{13}C$ [*eg., Curry and Oppo 2005; Duplessy 1988*].

2.2 Combined Mg/Ca and $\delta^{18}O$:

At present, the combination of Mg/Ca and $\delta^{18}O$ of foraminifera (and ostracods) has the most potential for reconstruction of Quaternary salinity changes and this combined method is beginning to be widely applied. Foraminiferal Mg/Ca provides an independent temperature estimate that can be used to extract the $\delta^{18}O_{water}$ signal from the $\delta^{18}O_{carbonate}$ record. Although there are a number of commonly used paleotemperature proxies, including alkenones, foraminiferal faunal assemblages, Mg/Ca of foraminifera and Sr/Ca of corals, all of which have their own advantages and disadvantages (reviewed in this volume), as a salinity proxy the combination of Mg/Ca and $\delta^{18}O$ has the advantage that both analyses are conducted on the same material (foraminiferal calcite), thus alleviating issues related to differences in seasonality, habitat and ecology.

Mg/Ca paleothermometry:

Although the relationship between Mg and temperature in calcite has been recognized for many years, Mg paleothermometry did not come widely into use until the last decade. Several early studies documented that magnesium was higher in foraminifera shells precipitated in warmer waters [*Bender, et al.*, 1975; *Chilingar*, 1962; *Hecht, et al.*, 1975; *Savin and Douglas*, 1973], although initial concerns about secondary effects precluded wide acceptance of the Mg/Ca proxy. However, studies of inorganic calcite precipitation demonstrated that magnesium incorporation is largely controlled by thermodynamics, and indicated that Mg substitution into the calcite lattice takes an exponential form that can be described by the equation:

$$Mg/Ca = b\ e^{mT}$$

Where b is the pre-exponential constant, m is the exponential constant and T is the temperature [*Katz*, 1973; *Mucci*, 1987; *Oomori, et al.*, 1987].

Mg/Ca temperature calibration equations

Since these early studies, work has focused on developing Mg-temperature calibration equations for biogenic calcites (benthic and planktonic foraminifera, ostracodes, molluscs) using culturing, sediment trap and core-top material. Calibration equations derived from live culturing experiments of *Globigerinoides sacculifer*, *Orbulina universa*, *Globigerina bulloides* and *Neogloboquadrina pachyderma* take an exponential form and indicate that these foraminifera species all incorporate Mg at a rate of approximately 10%/°C (exponential constants vary between 0.085 and 0.102; [*Lea, et al.*, 1999; *Mashiotta, et al.*, 1999; *Nürnberg, et al.*, 1996; *von Langen, et al.*, in press]. The pre-exponential constant, which determines the absolute temperature, ranges from 0.3 to 1.36, although all cultured species except *O. universa* fall in the range of 0.3 to 0.5. The reason for the large difference between *O. universa* and the other planktonic species is unknown, although O. universa is morphologically unique in its formation of a final spherical chamber. Mg-paleothermometry errors are on the order of 1.0-1.4°C. Core top and sediment trap studies are in good agreement with the culturing equations, and these studies have extended the calibration equations to additional planktonic species [*Anand, et al.*, 2003; *Elderfield and Ganssen*, 2000; *Hastings, et al.*, 1998; *Nürnberg*, 1995]. Although both tropical and temperate species have similar exponential constants, tropical species have lower pre-exponential constants than temperate and subpolar species [*von Langen, et al.*, in press]. (Figure 8).

The development of benthic foraminiferal calibration equations has lagged behind that of planktonic foraminifera, in part due to the difficulty in culturing these species, and the acquisition of live (*eg.,* rose-bengal stained) benthic formanifera from multi-cores or box cores with good sediment-water interfaces. *Rosenthal et al* [1997] defined a calibration equation for the epifaunal genus *Cibicidoides* between 5-18°C, which was extended to bottom water temperatures (<3°C) by *Martin et al.* [2002], yielding an exponential equation of

$$Mg/Ca=0.85^{.11BWT}$$

The standard error derived from the data set is 1.14°C. A study of Mg/Ca in other species of benthic foraminifera indicated that although several common species yielded results similar to that of *Cibicidoides*, the paleoceanographically important species *Uvigerina* apparently has a lower temperature sensitivity [*Lear, et al.*, 2002; *Martin, et al.*, 2002].

Mg/Ca paleothermometry has also been successfully applied to marine ostracodes [*Cronin, et al.*, 2000; *Dwyer, et al.*, 1995]. These small, benthic crustaceans secrete a calcite shell that incorporates Mg/Ca very similarly to foraminifera (approximately 9% per °C), although linear calibration equations have been applied [*Dwyer, et al.*, 1995].

Secondary effects

Because paleoceanographers are interested in isolating small temperature differences, it is important to accurately identify temperature changes. In addition to the temperature effect, the most prominent secondary effect on Mg/Ca in biogenic calcites is dissolution. Mg/Ca in shell calcite decreases with increasing dissolution on the seafloor. The cause of Mg loss is as yet uncertain, but may be due to inhomogenous distribution of Mg in shells and higher solubility of Mg-rich shell components. For instance, studies have shown that species with gametogenic calcite crusts or certain types of shell ornamentation, such as *N. dutertrei* or *G. tumida*, respectively, are more susceptible to Mg loss [*Brown and Elderfiel*d, 1996; *Rosenthal, et al.*, 2000; *Fehrenbach and Martin*, in review]. In order to have confidence in the Mg/Ca proxy it is necessary to either analyze only pristine shells, or to quantify the amount of dissolution and its effect on the Mg/Ca ratio. Dekens *et al.* [*Dekens, et al.*, 2002], analyzed Mg/Ca in three different planktonic species along Pacific and Atlantic depth transects in order quantify the percentage of Mg loss with depth increase, and developed dissolution-corrected calibration equations. For instance, for Pacific *G. ruber* the calibration equation is adjusted by 5% per kilometer depth. An alternative approach is to estimate the amount of post-depositional dissolution by measuring average shell masses and normalizing Mg/Ca ratios accordingly [*Rosenthal and Lohmann*, 2002].

Foraminiferal culturing experiments have been done to quantify the effects of salinity and pH on Mg/Ca. These studies indicate that although temperature is the dominant control, both salinity and pH exert a minor influence on shell Mg/Ca. For *G. bulloides* and *O. universa*, shell Mg/Ca decreases 6% per 0.1 pH unit. Salinity exerts a smaller influence of approximately 4% per psu in *O. universa* [*Lea, et al.*, 1999; *Sanyal, et al.*, 1996].

3. *Quaternary $\delta^{18}Ow$ Variations an Example from the Tropical Pacific:*

As an example of the combined Mg/Ca and δ^{18}O technique we highlight the work of *Lea et al.*, [2002] from the equatorial Pacific. We first focus on TR163-19 (2°N, 91°W) near the Galapagos in the eastern Pacific (Figure 9). Oxygen isotope measurements of the surface dwelling planktonic foraminifera *Gs. ruber* exhibit the characteristic "saw-tooth" pattern observed in most if not all Quaternary δ^{18}O profiles. The glacial interglacial difference in $\delta^{18}O_{carbonate}$ is ~1.8‰. Mg/Ca concentrations on the same species of planktonic foraminifera are interpreted to reflect a glacial-interglacial sea surface temperature (SST) difference on the order of ~2.6°C. If we strictly interpret the Mg/Ca results as SST and convert the temperature difference into δ^{18}O space we can then subtract the "SST" signature from the observed $\delta^{18}O_{carbonate}$. This yields a predicted $\delta^{18}O_{water}$time-series (estimated error ± ~0.2‰) that includes glacial (eustatic) and local/regional $\delta^{18}O_w$ differences. The difference during the last glacial maximum is ~1.2‰ which if the whole ocean were heavier by ~1‰ leaves ~0.2‰. If the glacial salinity-$\delta^{18}O_{water}$relationship were similar to today's, this difference implies an ~1psu increase either by reduced rainfall or a stronger influence of subtropical surface waters brought to the equator in the North Equatorial Current. Given the location of the core relative the modern day Inter-tropical convergence zone (ITCZ) a southward displacement of the ITCZ would allow for more subtropical water to gain influence over the site. Clearly apparent in the time-series is the fact that tropical SST leads $\delta^{18}O_{water}$ by ~3kyr, particularly on transitions to interglacial periods.

Because of questions regarding the exact history of eustatic (glacial) $\delta^{18}O_{water}$ and the lack of a standardized curve (where at least every use would be working with the same record) *Lea et al.,* [2002] like many others do not explicitly subtract out an ice volume component. Instead *Lea et al*., [2002] use a "site to site" comparison with ODP 806, a core from the western equatorial (0°, 159°E) Pacific warm pool (Figure 10). The site to site comparison assumes that the ice volume signal is common in each record and therefore differences between the two $\delta^{18}O_{water}$ records are a reflection of changes in local salinity ($\delta^{18}O_{water}$). In the western Pacific the $\delta^{18}O_{water}$ glacial-interglacial amplitude is only ~0.75‰ and less than that expected due to ice volume. This observation requires that the surface waters overlying ODP 806 had a more negative $\delta^{18}O_{water}$ than today and most likely were also less saline. In combination with the results from TR163-169 the ODP 806 results indicate a different surface water $\delta^{18}O_{water}$ gradient in the tropical Pacific during glacials with the east being more positive and the west being more negative. An additional feature in both records, and especially in that of ODP806, is what appears to be a long-term secular trend in $\delta^{18}O_{water}$ on the order of ~0.1‰/kyr. If not an artifact, such a trend could indicate a larger glacial sea level drop earlier in the record (*ie.,* MIS 12) and or a change in the mean $\delta^{18}O$ of glacial ice.

Where does $\delta^{18}O_{water}$ reconstructions stand? The signals that we would like to directly interpret are small and there have been inconsistencies when one study applies a calibration from one lab to another set of results or species measured by a different technique. The observation of inter-laboratory offsets has necessitated standardization of Mg/Ca techniques [*c.f. Rosenthal et al* 2002; *Lea et al*., 2002]. Consistently applied error propagation is necessary so that one can gauge the validity of any single down-core result: ideally we want to be able to interpret sub-millennial variability when the sedimentary-depositional environment allows us to. To remove the ice volume component from the estimated $\delta^{18}O_{water}$ requires at the very least, a common internationally agreed upon standard Quaternary sea-level record and ice volume ($\delta^{18}O$) scaling.

Acknowledgements: We thank Dave Anderson for the opportunity to contribute to this encyclopedia, and Kate Newell for her patience and diligence. We would particularly like to thank Pamela Martin for comments, criticisms, and timely suggestions. A portion of this work was performed under the auspices of the U.S. Department of Energy by the University of California Lawrence Livermore National Laboratory (contract W-7405-Eng-48

References

Adkins, J. F., K. McIntyre, and D. P. Schrag (2002), The salinity, temperature, and 18O of the glacial deep ocean, *Science*, 298, 1789-1773.

Anand, P., et al. (2003), Calibration of Mg/Ca thermometry in planktonic foraminifera from a sediment trap time series, *Paleoceanography*, *18 (2)*, doi:10.1029/2002PA000846, 002003.

Bemis, B. E., H. J. Spero, J. Bijma and D. W. Lea (1998) Reevaluation of the oxygen isotopic composition of planktonic foraminifera: Experimental results and revised paleotemperature equations. *Paleoceanography* 13(2): 150-160.

Bender, M. L., et al. (1975), Sodium, magnesium, and strontium in the tests of planktonic foraminifera, *Micropaleo.*, *21*, 448-459.

Broecker, W.S., and T-H Peng (1982), *Tracers in the Sea* ELDIGIO Press, Palisades NY

Brown, S., and H. Elderfield (1996), Variations in Mg/Ca and Sr/Ca ratios of planktonic foraminifera caused by postdepositional dissolution - evidence of shallow Mg-dependent dissolution., Paleoceanography, 11, 543-551.

Chilingar, G. V. (1962), Dependence on temperature of Ca/Mg ratio of skeletal structures of organisms and direct chemical precipitates out of sea water, *Bulletin of the Southern California Academy of Sciences*, *61*, 45-61.

Craig, H., and L. I. Gordon (1965), Deuterium and oxygen-18 variations in the ocean and the marine atmosphere, in *Stable Isotopes in Oceanographic Studies and Paleotemperatures,* Soleto, July 26-27, 1965, Consiglio Nazionale delle Richerche, Laboratorio di Geologia Nucleare, Pisa, 1-22.

Cronin, T. M., et al. (2000), Orbital and suborbital variability in North Atlantic bottom water temperature obtained from deep-sea ostracod Mg/Ca ratios, *Palaeogeography, Palaeoclimatology, Palaeoecology*, *162*, 45-57.

Curry, W. B. and D. W. Oppo (2005), Glacial water mass geometry and the distribution of δ^{13}C of ΣCO2 in the western Atlantic Ocean, *Paleoceanography*, 20, PA1017, doi:10.1029/2004PA001021.

Dansgaard, W., (1964), Stable isotopes in precipitation. *Tellus*, 16, 436-468.

Dekens, P., et al. (2002), A core-top calibration of Mg/Ca in tropical foraminifera: Refining paleo-temperature estimation, *Geochem. Geophys. Geosys.*, *8.*

Duplessy, J. C., *et al.*, (1988), Deep water source variations during the last climatic cycle and their impact on the global deepwater circulation. *Paleoceanography*, 3, 343-360.

Dwyer, G. S., et al. (1995), North Atlantic deepwater temperature change during Late Pliocene and Late Quaternary climatic cycles, *Science*, *270*, 1347-1351.

Elderfield, H., and G. Ganssen (2000), Past temperature and δ^{18}O of surface ocean waters inferred from foraminiferal Mg/Ca ratios, *Nature*, *4005*, 442-445.

Epstein , S., *et al.*., (1951), Carbonate-water isotopic temperature scale. *Bull. of the Geol. Soc. of Amer.*, 62, 417-426.

Epstein, S., *et al.*, (1953), The revised carbonate-water oxygen isotope paleotemperature scale. *Geol. Soc. Amer. Bull* ., 64, 1315-1326.

Faure, G., (1986) *Principles of Isotope Geology*, John Wiley and Sons.

Fairbanks, R. G., and R. K. Matthews, (1978), The marine oxygen isotope record in Pleistocene coral, Barbados, West Indies. *Quat. Res.*, 10, 181-196.

Fairbanks, R. G. (1989), A 17,000 year glacio-eustatic sea level record: Influence of glacial melting rates on the Younger Dryas event and deep-ocean circulation, *Nature*, 342, 637-642.

Fairbanks, R. G. (1990), The age and origin of the 'Younger Dryas climate event' in Greenland ice cores, *Paleoceanography*, 5(6):937-948.

Fairbanks, R. G., C. D. Charles, and J. D. Wright, (1992) Origin of global meltwater pulses. In: Taylor, R.E., *et al.*, (eds) *Radiocarbon After Four Decades*. Springer-Verlag. 473-500.

Hastings, D. W., et al. (1998), Foraminiferal magnesium in *Globeriginoides sacculifer* as a paleotemperature proxy, *Paleoceanography*, *13*, 161-169.

Hecht, A. D., et al. (1975), Experimental studies on the dissolution of planktonic foraminifera, in *Dissolution of Deep-Sea Carbonates*, edited, pp. 59-69, Cushman Foundation for Foraminiferal Research.

Hendy, E. J. et al. (2002). Abrupt shift in tropical sea surface salinity at end of Little Ice Age. *Science*, 295,1511-1514.

Imbrie, J. I., and N. G. Kipp, (1971), A new micropaleontological method for quantitative paleoclimatology: Application to a late Pleistocene Caribbean core. In: Turekian, K. K., (ed)., *The late Cenozoic glacial ages*. Yale University Press, New Haven, Conn., 71-181.

Joreskog, K. G., J. E. Klovan, and R. A. Reyment (1976), *Geological Factor Analysis*. Elsevier 178pp.

JPOTS (1980), The practical salinity scale 1978 and the international equation of state of seawater. Paris, UNESCO 25pp.

Katz, A. (1973), The interaction of magnesium with calcite during crystal growth at 25-90°C and one atmosphere, *Geochim. Cosmochim. Acta*, *37*, 1563-1586.

Kim, S. T., and J. R. O'Neil (1997), Equilibrium and non-equilibrium oxygen isotope effects in synthetic carbonates. *Geochimica et Cosmochimica Acta*, 61, 3461-3475.

Kipp, N. G., (1976), New Transfer Function for Estimating Past Sea-Surface Conditions from Sea-Bed Distribution of Planktonic Foraminiferal Assemblages in the North Atlantic. *Geologial Society of America Memoir* 145, 3-41.

Lea, D. W., et al. (1999), Controls on magnesium and strontium uptake in planktonic foraminifera determined by live culturing, *Geochim. Cosmochim. Acta*, *63*, 2369-2379.

Lear, C., et al. (2002), Benthic foraminiferal Mg/Ca-paleothermometry: A revised core-top calibration, *Geochimica et Cosmochimica Acta*, *66*, 3375-3387.

Martin, P. A., et al. (2002), Quaternary deep sea temperature histories derived from benthic foraminiferal Mg/Ca, *Earth and Planetary Science Letters*, *198*, 193-209.

Mashiotta, T. A., et al. (1999), Glacial-interglacial changes in Subantarctic sea surface temperature and δ^{18}O-water using foraminiferal Mg, *Earth Planet. Sci. Lett.*, *170*, 417-432.

Maslin, M. A., and S. J. Burns (2000), Reconstruction of the Amazon Basin effective moisture availability over the past 14,000 years. *Science*, 290, 2285-2287.

McCrea, J. M., (1950), On the isotopic chemistry of carbonates and a paleotemperature scale. *J. of Chem. Phys.*, 6, 849-857.

McCulloch, M. T. et al. (1994), A high resolution Sr/Ca and δ^{18}O coral record from the Great Barrier Reef, Australia, and the 1982-1983 El Nino. *Geochim et Cosmochim Acta,* 58, 2747-2754.

Millero, F. J. (1996), *Chemical Oceanography* (2nd ed). New York, CRC Press.

Mix, A. C. (1987), The oxygen-isotope record of glaciation, in Ruddiman, W. F., and H. E. Wright Jr., (eds.), *North America and adjacent oceans during the last deglaciation* Boulder, Colorado, Geological Society of America, Geology of North America, v. K-3, p. 111-135.

Mucci, A. (1987), Influence of temperature on the composition of magnesian calcite overgrowths precipitated from seawater, *Geochim. Cosmochim. Acta*, *51*, 1977-1984.

Nürnberg, D. (1995), Magnesium in tests of *Neogloboquadrina pachyderma* sinistral from high Northern and Southern latitudes, *J. Foram. Res.*, *25*, 350-368.

Nürnberg, D., et al. (1996), Assessing the reliability of magnesium in foraminiferal calcite as a proxy for water mass temperatures, *Geochim. Cosmochim. Acta*, *60*, 803-814.

Oomori, T., et al. (1987), Distribution coefficient of Mg^{2+} ions between calcite and solution at 10-50°C, *Mar. Chem.*, *20*, 327-336.

Prell, W. L., and J. D. Hays (1976), Late Pleistocene Faunal and Temperature Patterns of the Colombia Basin, Caribbean Sea. *Geological Society of America Memoir* 145, 201-220

Rosenthal, Y., and G. P. Lohmann (2002), Accurate estimation of sea surface temperatures using dissolution-corrected calibrations for Mg/Capaleothermometry, *Paleoceanography*, *17*, doi:10.1029/2001PA000749.

Rosenthal, Y., et al. (2000), Incorporation and preservation of Mg in *Globigerinoides sacculifer*: implications for reconstructing the temperature and $^{18}O/\ ^{16}O$ of seawater, *Paleoceanography*, *15*, 135-145.

Rozanski, K., L. Araguas-Araguas, and R. Gonfiantini (1993) Isotopic patterns in modern global precipitation. In P. K. Swart, K. C. Lohman, J. McKenzie and S. Savin (eds.) *Climate Change in Continental Isotopic Records - Geophysical Monograph* 78, American Geophysical Union, Washington, D.C., p. 1-36.

Sanyal, A., et al. (1996), Oceanic pH control on the boron isotopic composition of foraminifera: Evidence from culture experiments, *Paleoceanography*, *11*, 513-517.

Savin, S. M., and R. G. Douglas (1973), Stable isotope and magnesium geochemistry of recent planktonic foraminifera from the south Pacific, *Geol. Soc. Am. Bull.*, *84*, 2327-2342.

Schmidt, G.A., G. R. Bigg and E. J. Rohling (1999), *Global Seawater Oxygen-18 Database* data.giss.gov/data/

Schrag, D., G. Hampt, and D. W. Murray, (1996), Pore fluid constraints on the temperature and oxygen isotopic composition of the glacial ocean. *Science*, 272, 1930-1932.

Shackleton, N. J. (1974), Attainment of isotopic equilibrium between ocean waters and the benthonic foraminifera genus Uvigerina: Isotopic changes in the ocean during the last glacial. *Cent. Nat. Rech., Sci. Colloq. Inst.* 219, 203-209.

Spero, H. J., J. Bijma, D. W. Lea and B.E. Bemis (1997), Effect of seawater carbonate concentration on planktonic foraminiferal carbon and oxygen isotopes. *Nature,* 390, 497-500.

Urey, H., (1947), The thermodynamic properties of isotopic substances. *J. Chem Soc.,* 1, 562-581.

Urey, H. C., *et al.*, (1951), Measurement of paleotemperatures and temperatures of the Upper Cretaceous of England, Denmark, and the southeastern United States. *Geol. Soc. Amer. Bull.*, 62, 399-416.

von Langen, P., et al. (in press), Effects of temperature on Mg/Ca in neogloboquadrinid shells determined by live culturing, *Geochemistry, Geophysics, Geosystems.*

Weber, J. N., and P. M. J. Woodhead, (1972),Temperature Dependence of Oxygen-18 Concentration in Reef Coral Carbonates. *J. Geophys. Res.*, 77(3), 463-473.

Wooster W. S., A. J. Lee, and G. Dietrich (1969), Redefinition of salinity. *Deep-Sea Research* 16, 321–322.

Figure Captions

Figure 1. Western Atlantic salinity (psu) profile as a function of latitude and depth (m) observed during the GEOSECS expedition.

Figure 2. Relationship between potential temperature (°C), salinity (psu), and sea water potential density (σt: kg-m^{-3}). Representative values for the three main interior water masses in the Atlantic basin are shown.

Figure 3. A cartoon representation of the "Imbrie-Kipp" transfer function technique (*cf.*, Fig 1 of *Kipp* [*1979*]). Relative abundance of foraminifera species and/or morphotypes determined from faunal census counts of the >125*μ* size fraction with at least 300 individuals counted per sample. Benthic forams and/or foram fragments are also counted and used as a proxy for preservation. Data may be "row normalized" and the relative abundances are decomposed via (Q-Mode) empirical orthogonal factor analysis. Depending on the type of analysis one is attempting to relate spatial patterns of abundance or "commonality" of the relative abundances. In practice, the decomposition of global core-top databases yields 5-7 major "factors" or the analysis can be basin specific. The resulting factors are in essence regressed via a multiple-linear regression against environmental variables (*eg.,* salinity) which then provides a "key" to transform down-core species assemblages back into an environmental variable. In concept, the modern analog technique is similar but seeks to relate the factors directly back to environmental variables without a regression algorithm.

Figure 4. Transfer function based surface salinity estimate from the Columbian Basin (after *Prell and Hays, [1976]*) through marine isotope stage 6. Left vertical axis is depth down core (metres) and corresponding carbonate (isotope) stage designations is provided on the right.

Figure 5. a) Mean annual δ^{18}O of precipitation as a function of latitude (°N) and altitude, an update using the IAEA ISOHIS database to figures originally reported in *eg., Dansgaard* 1964; *Rozanski et al.*, 1992 among others. b) Cartoon schematic of the effect of a growing ice-sheet on mean ocean δ^{18}O.

Figure 6. a) Surface water salinity versus δ^{18}O (‰) in the Pacific and representative deep-ocean values (redrawn after *Craig and Gordon, [1965]*). b) Relationship between 0-10metre salinity and surface ocean δ^{18}O (‰) for all surface waters (data from the online data base of *Schmidt et al.*, [1999]). Note the different "zero-salinity" end-members and the corresponding changes in slope. c) Atlantic surface water salinity-δ^{18}O relationships (redrawn after *Fairbanks et al.*, [*1992*]).

Figure 7. Last glacial maximum salinity (psu) and potential temperature (°C) as estimated from pore-water chlorinity, δ^{18}O pore-waters, and benthic foraminiferal δ^{18}O at four ODP core sites. The stippled regions represent propagated error ranges, and curved lines denote lines of constant density (σ4) during the last glacial maximum. The arrows demark mean ocean salinity for present (~34.7) and during the glaciation (~35.9).

Present day values/estimates for the core locations are also shown. Redrawn after *Adkins et al.*, [2002].

Figure 8. A composite of planktonic foraminifera temperature (°C) versus Mg/Ca (mmol/mole) "calibrations".

Figure 9. a) TR163-19, eastern equatorial Pacific downcore *Gs. ruber* $\delta^{18}O$ (‰- blue) and Mg/Ca (mmol/mole and SST°C estimate – red). b) Deconvolved $\delta^{18}O_{water}$ (‰ – blue) and Mg/Ca-SST (°C - red) using the data of a. Data from *Lea et al.*, [2002].

Figure 10. A comparison of Quaternary (0-450 kyrBP) planktonic foraminifera surface $\delta^{18}O_{water}$ (‰) reconstructions from the western (ODP 806; solid blue) and eastern (TR163-19; dotted red) equatorial Pacific. To minimize noise the individual data were passed through a triangle filter, and data have not had a sea level $\delta^{18}O$ correction applied. Redrawn after *Lea et al.*, [2002]. Core top $\delta^{18}O_{water}$ estimates are consistent with modern day observations.

Figure 1

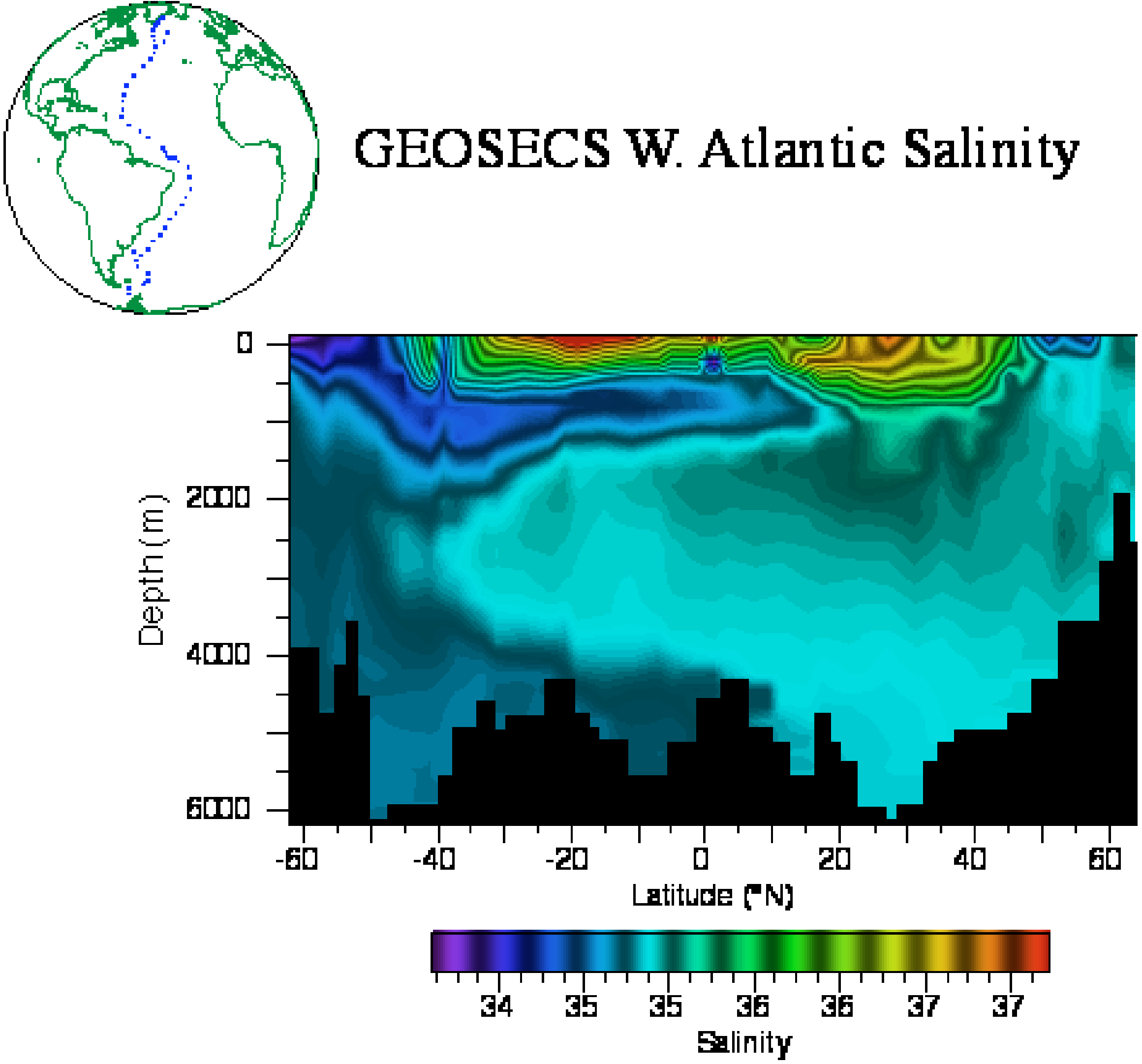
GEOSECS W. Atlantic Salinity
0
2000
4000
6000
Depth (m)
-60
-40
-20
0
20
40
60
Latitude (°N)
34
35
35
36
36
37
37
Salinity

Figure 2

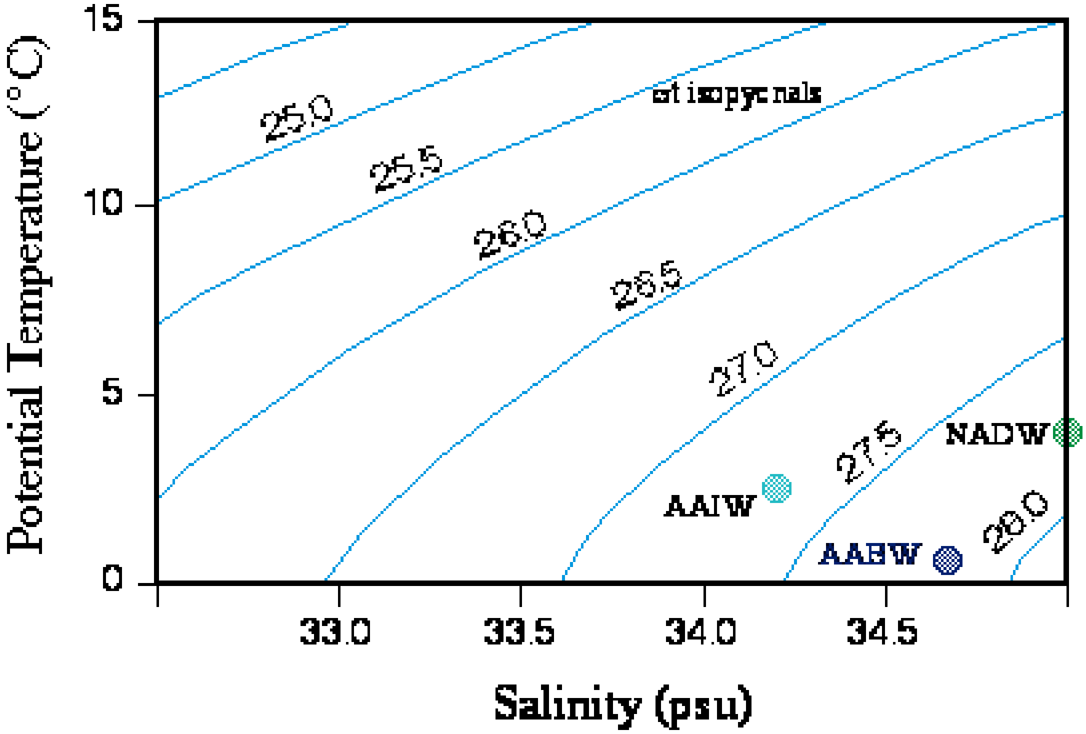

15
10
5
0
Potential Temperature (°C)
σt isopycnals
25.0
25.5
26.0
26.5
27.0
27.5
28.0
NADW
AAIW
AABW
33.0
33.5
34.0
34.5
Salinity (psu)

Figure 3

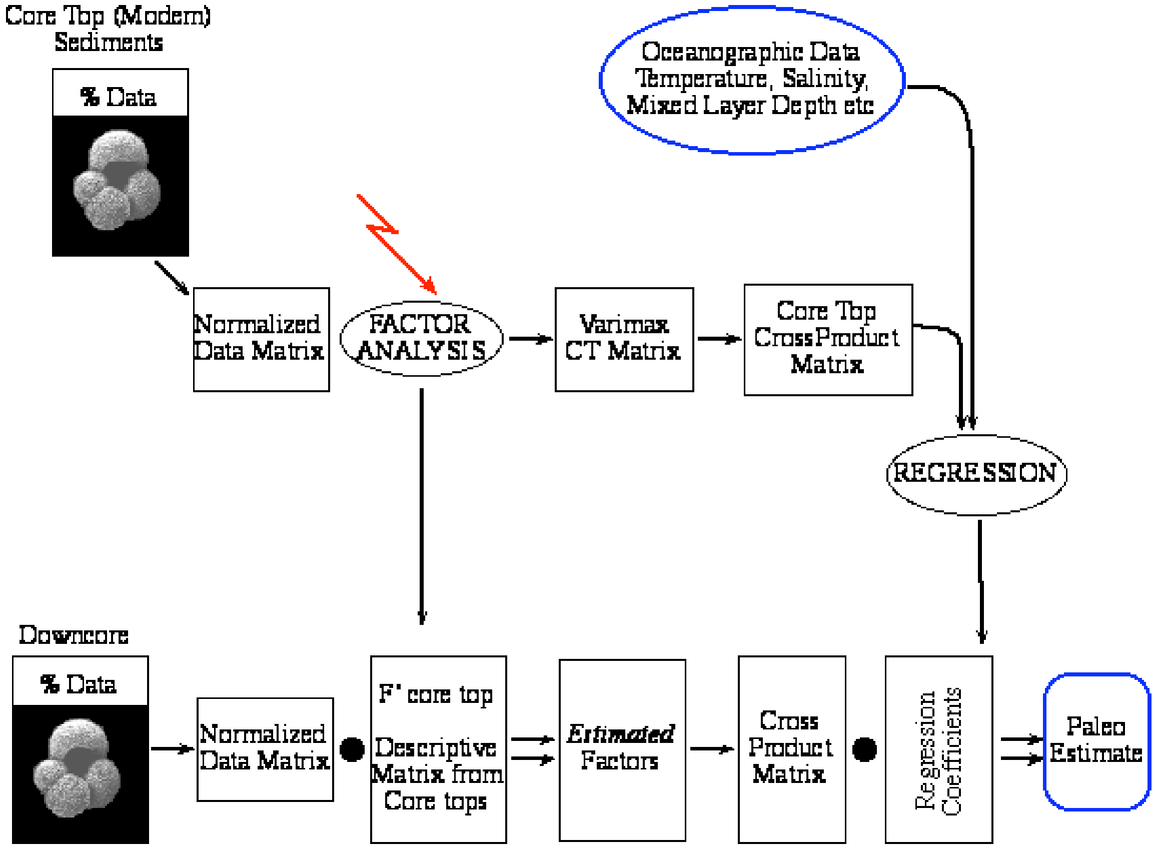
Core Top (Modern) Sediments
% Data
Oceanographic Data
Temperature, Salinity,
Mixed Layer Depth etc
Normalized Data Matrix
FACTOR ANALYSIS
Varimax CT Matrix
Core Top CrossProduct Matrix
REGRESSION
Downcore
% Data
Normalized Data Matrix
F' core top
Descriptive Matrix from Core tops
Estimated Factors
Cross Product Matrix
Regression Coefficients
Paleo Estimate

Figure 4

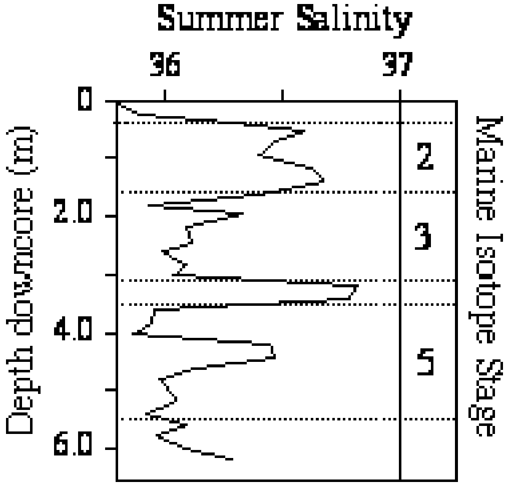
Summer Salinity
36
37
0
2.0
4.0
6.0
Depth downcore (m)
2
3
5
Marine Isotope Stage

Figure 5a

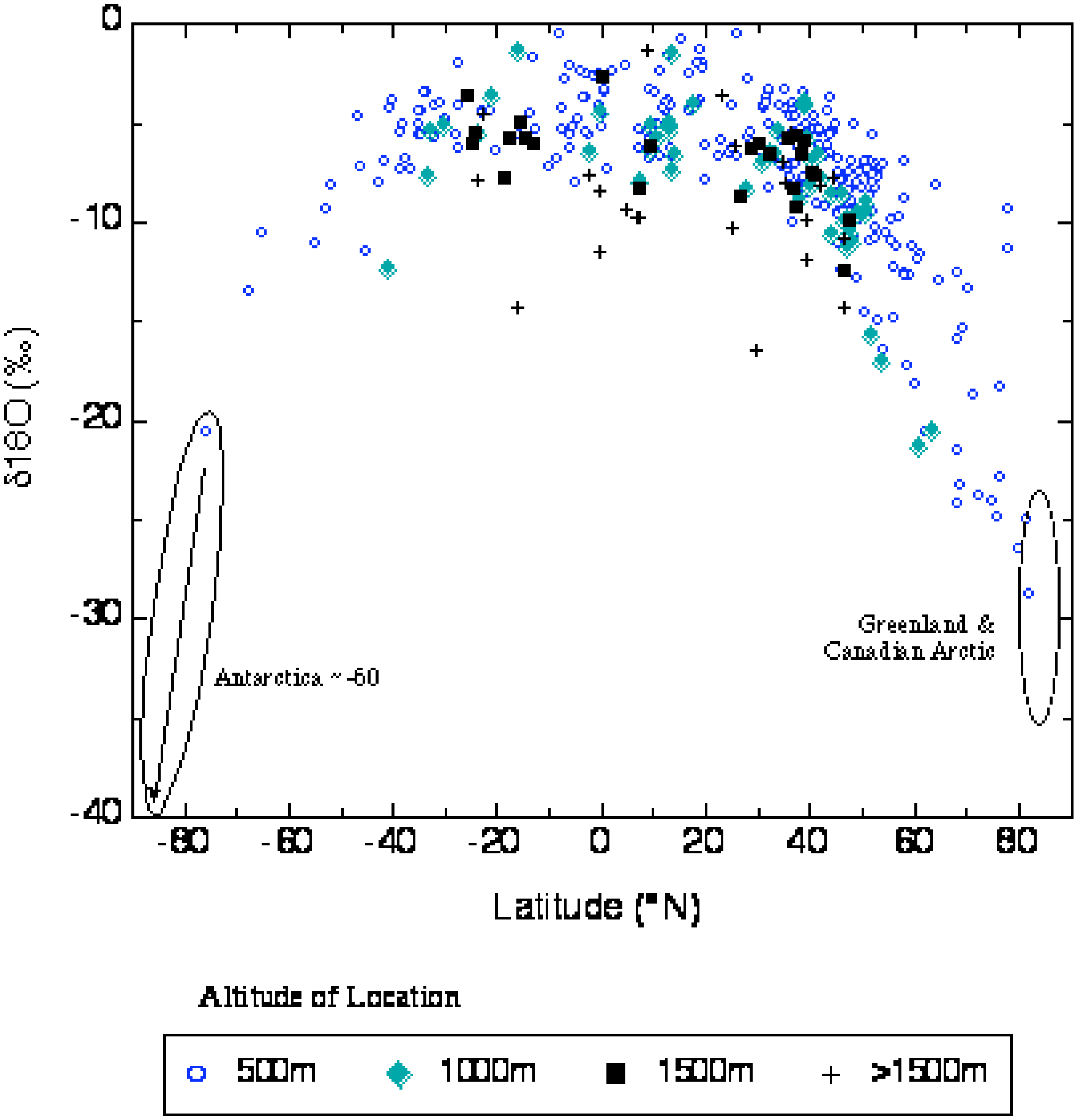
0
-10
-20
-30
-40
δ18O (‰)
-80
-60
-40
-20
0
20
40
60
80
Latitude (°N)
Antarctica ~-60
Greenland &
Canadian Arctic
Altitude of Location
○ 500m
◆ 1000m
■ 1500m
+ >1500m

Figure 5b

Relationship between sea level, glacial ice, and $\delta^{18}O$ sea water

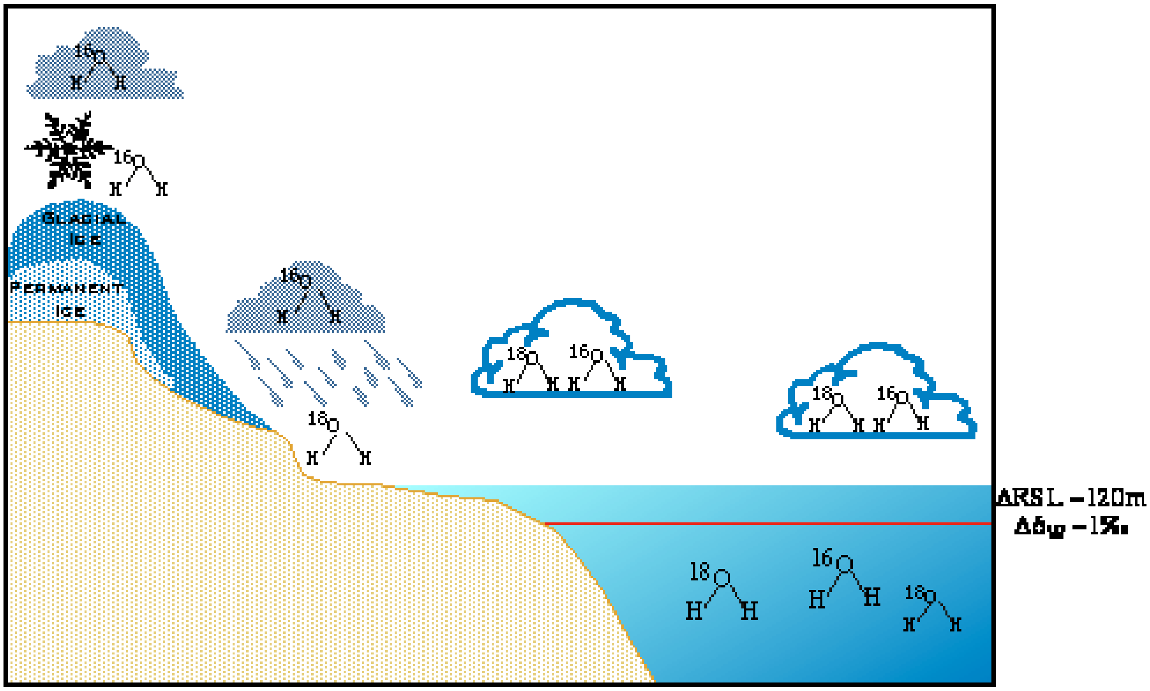
^{16}O H H
^{16}O H H
GLACIAL ICE
PERMANENT ICE
^{16}O H H
^{18}O H H
^{18}O H H ^{16}O H H
^{18}O H H ^{16}O H H
ΔRSL −120m
$\Delta\delta_w$ −1‰
^{18}O H H
^{16}O H H
^{18}O H H

Figure 6a

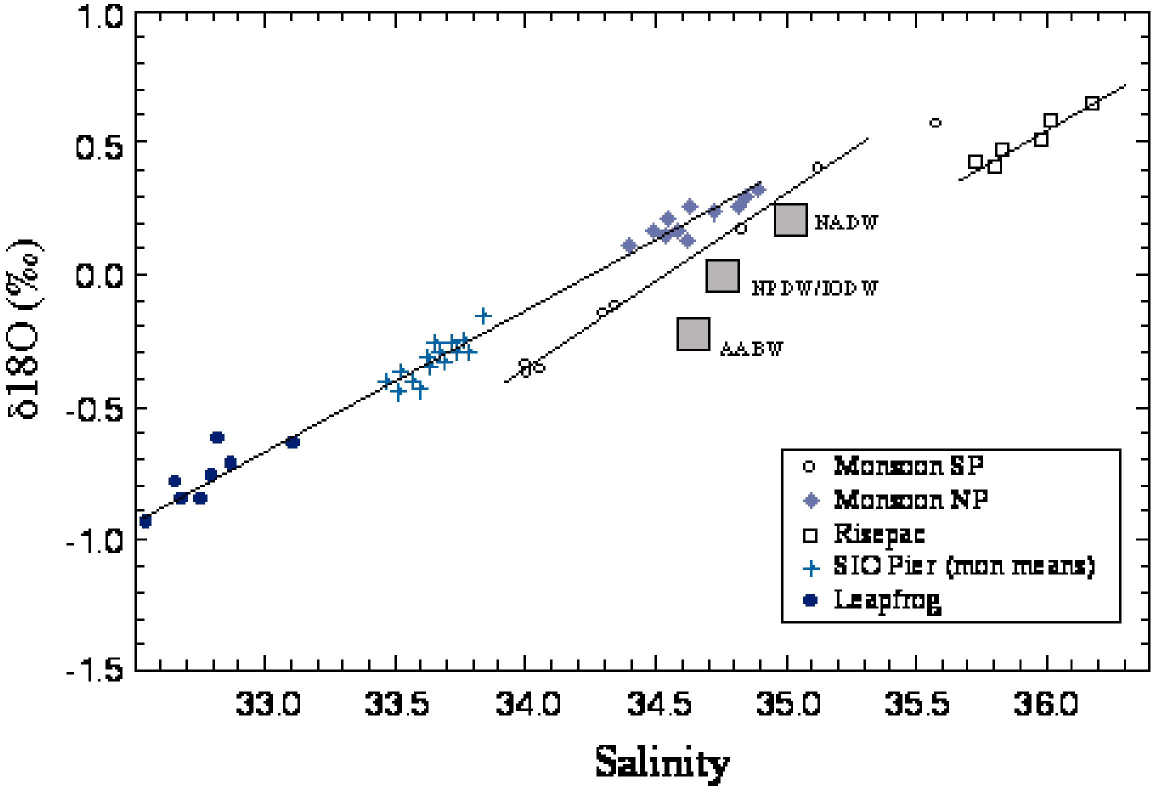

1.0
0.5
0.0
-0.5
-1.0
-1.5
δ18O (‰)
33.0
33.5
34.0
34.5
35.0
35.5
36.0
Salinity
NADW
NPDW/IODW
AABW
Monsoon SP
Monsoon NP
Risepac
SIO Pier (mon means)
Leapfrog

Figure 6b

Global Surface (0-10m) Salinity - δ18Ow

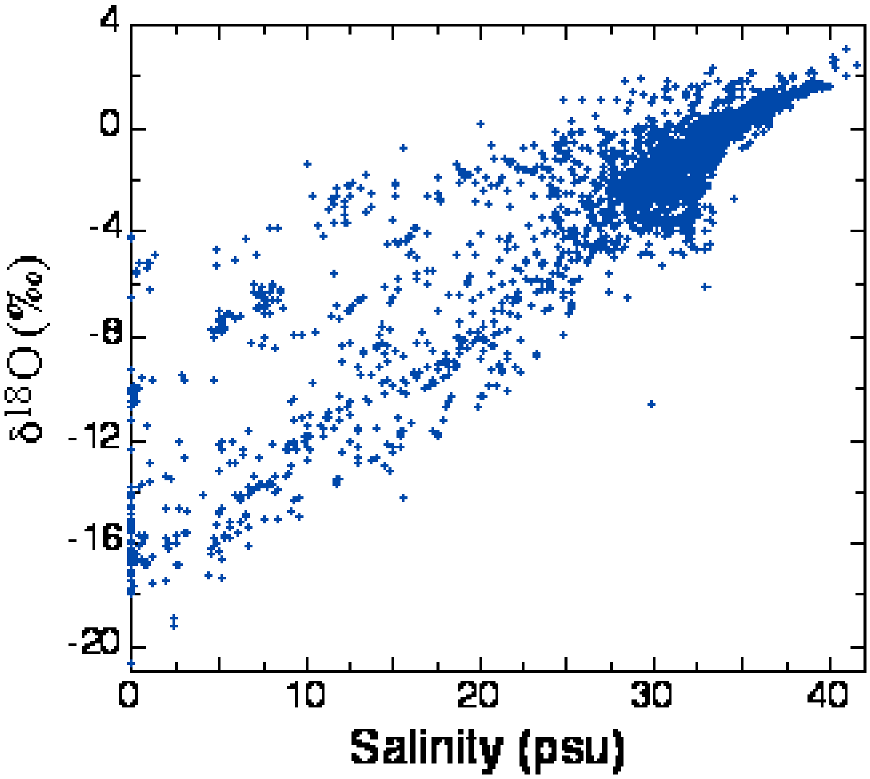

Figure 6c

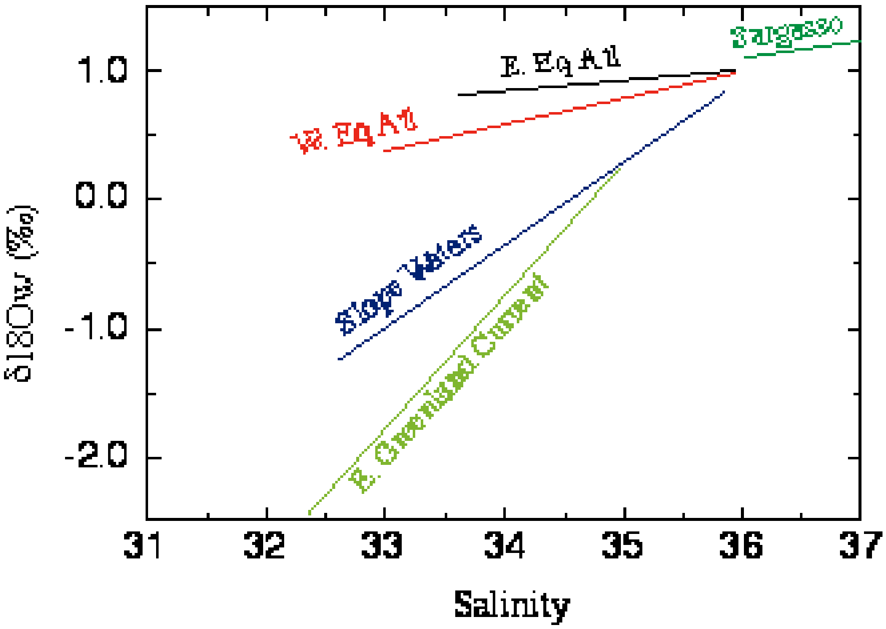

Sargasso
E. Eq Atl
W. Eq Atl
Slope Waters
E. Greenland Current
1.0
0.0
-1.0
-2.0
δ18Ow (‰)
31
32
33
34
35
36
37
Salinity

Figure 7

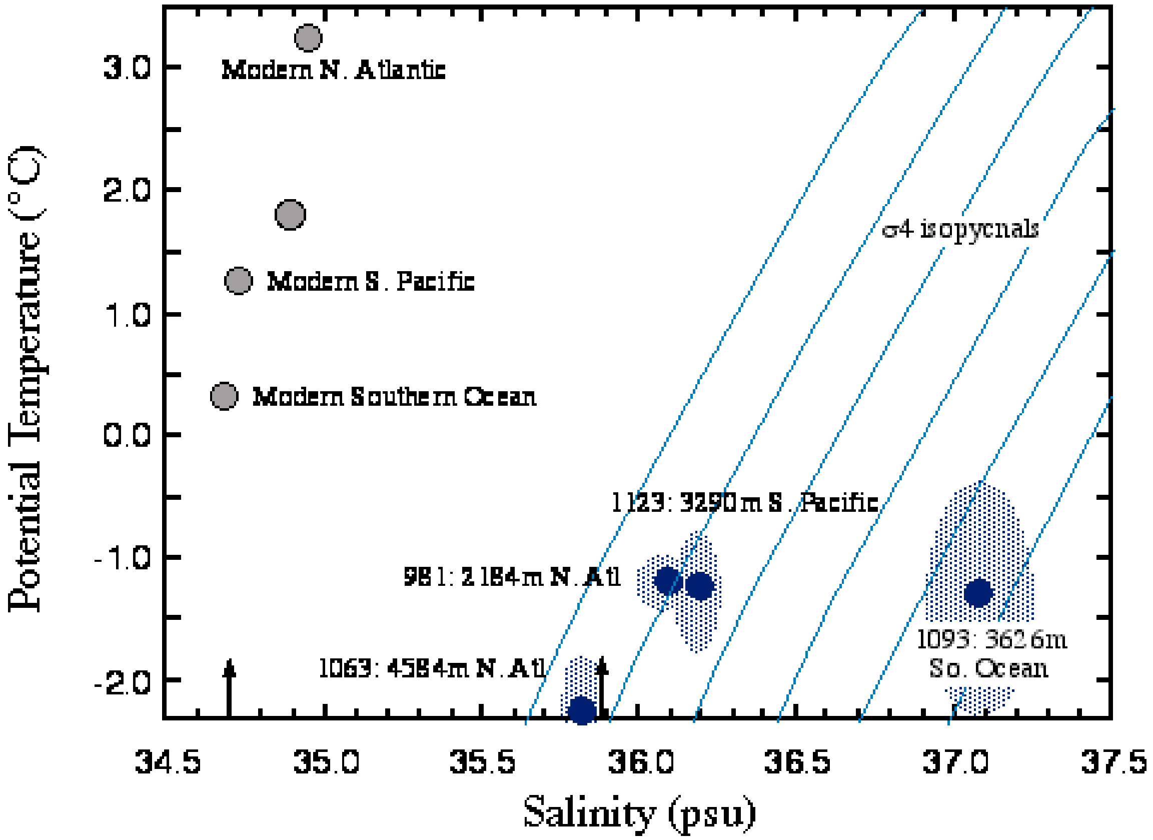

Modern N. Atlantic
Modern S. Pacific
Modern Southern Ocean
σ4 isopycnals
1123: 3290m S. Pacific
981: 2184m N. Atl
1063: 4584m N. Atl
1093: 3626m
So. Ocean
3.0
2.0
1.0
0.0
-1.0
-2.0
34.5
35.0
35.5
36.0
36.5
37.0
37.5
Potential Temperature (°C)
Salinity (psu)

Figure 8

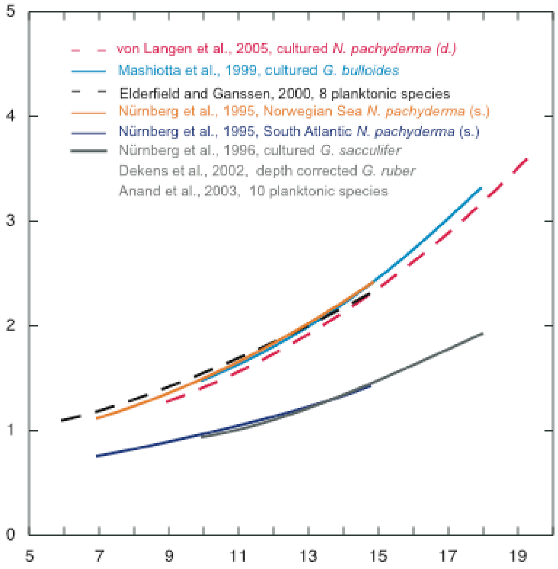

Figure x

Figure 9

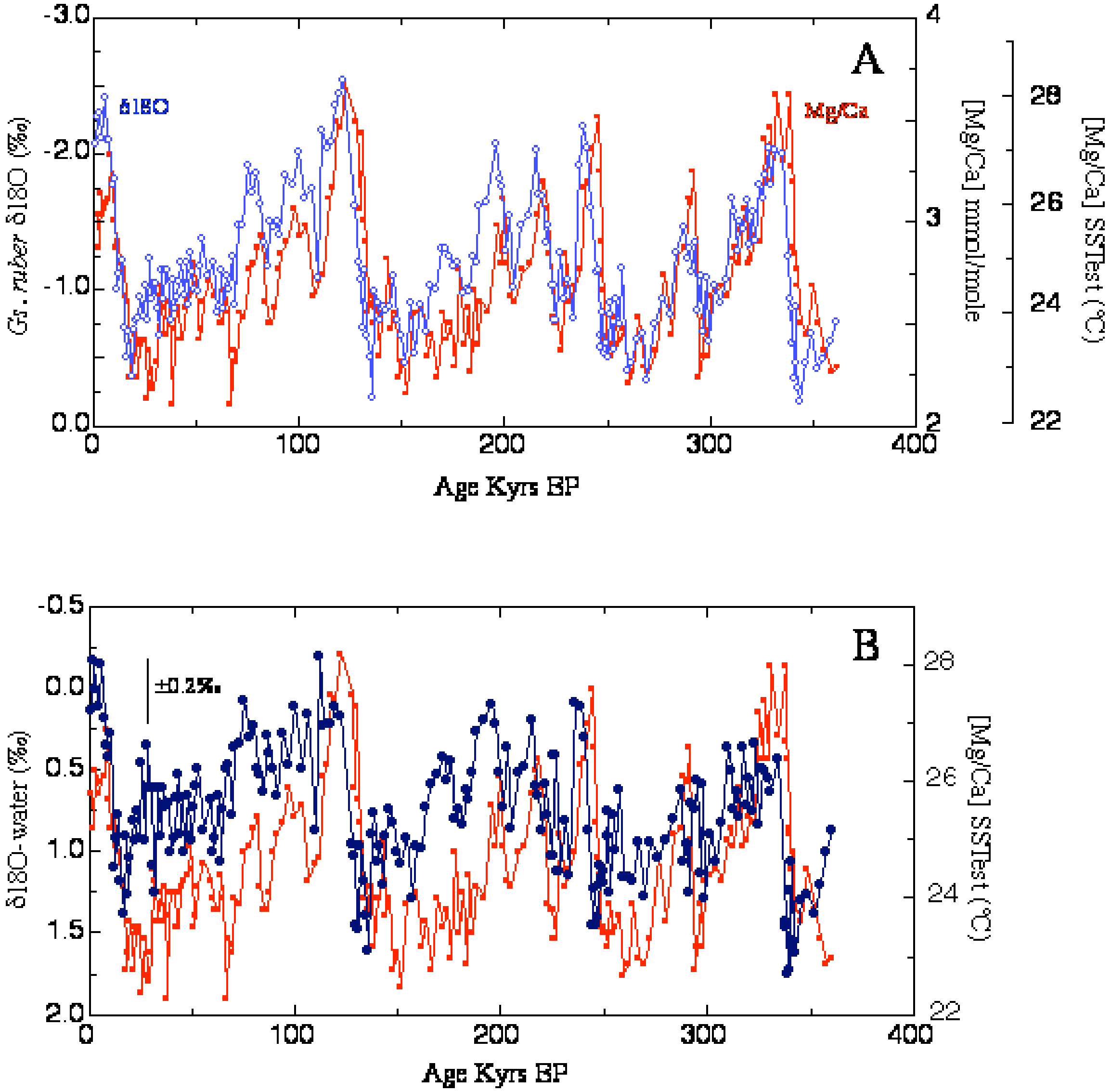

A
-3.0
-2.0
-1.0
0.0
Gs. ruber δ18O (‰)
δ18O
Mg/Ca
4
3
2
[Mg/Ca] mmol/mole
28
26
24
22
[Mg/Ca] SSTest (°C)
0
100
200
300
400
Age Kyrs BP
B
-0.5
0.0
0.5
1.0
1.5
2.0
δ18O-water (‰)
±0.2‰
28
26
24
22
[Mg/Ca] SSTest (°C)
0
100
200
300
400
Age Kyrs BP

Figure 10.

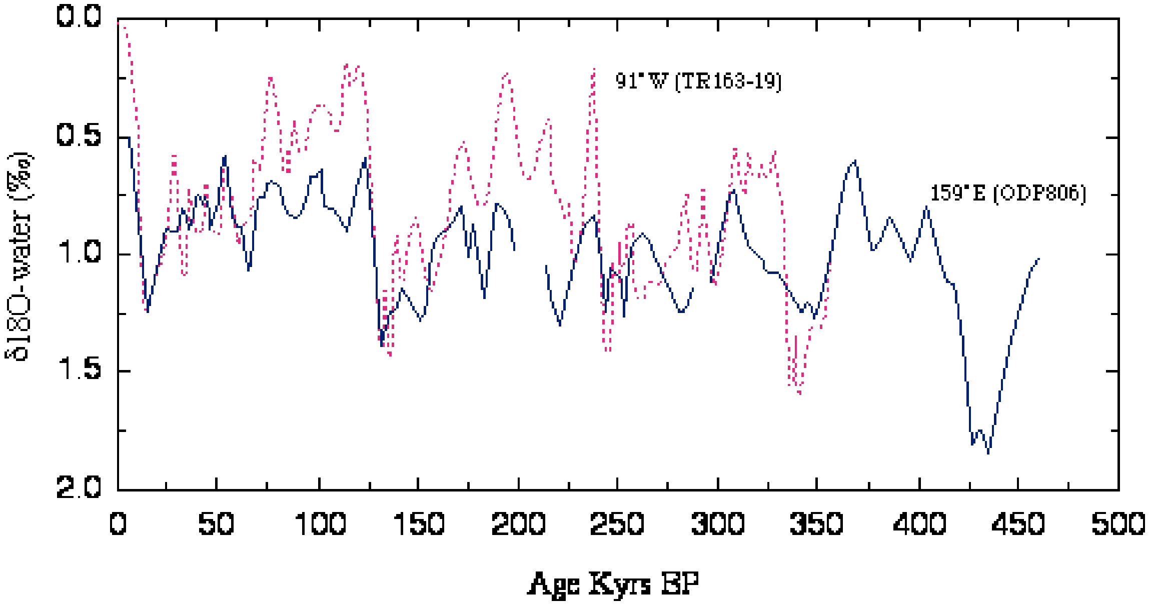

0.0
0.5
1.0
1.5
2.0
δ18O-water (‰)
0
50
100
150
200
250
300
350
400
450
500
Age Kyrs BP
91° W (TR163-19)
159° E (ODP806)